INFECTION AND IMMUNITY, Dec. 2003, p. 7023–7034 Vol. 71, No. 12
0019-9567/03/$08.00+0 DOI: 10.1128/IAI.71.12.7023–7034.2003

In Situ Study of Abundant Expression of Proinflammatory Chemokines and Cytokines in Pulmonary Granulomas That Develop in Cynomolgus Macaques Experimentally Infected with *Mycobacterium tuberculosis*

Craig L. Fuller,[1] JoAnne L. Flynn,[2] and Todd A. Reinhart[1]*

Department of Infectious Diseases and Microbiology, Graduate School of Public Health,[1] and Department of Molecular Genetics and Biochemistry, School of Medicine,[2] University of Pittsburgh, Pittsburgh, Pennsylvania

Received 25 April 2003/Returned for modification 17 June 2003/Accepted 20 August 2003

Tuberculosis remains a major public health problem worldwide. Chemokines and cytokines organize and direct infiltrating cells to sites of infection, and these molecules likely play crucial roles in granuloma formation and maintenance. To address this issue, we used in situ hybridization (ISH) to measure chemokine and cytokine mRNA expression levels and patterns directly in lung tissues from cynomolgus macaques (*Macaca fascicularis*) experimentally infected with a low dose of virulent *Mycobacterium tuberculosis*. We examined more than 300 granulomas and observed abundant expression of gamma interferon (IFN-γ)-inducible chemokine mRNAs (CXCL9/monokine induced by IFN-γ, CXCL10/IFN-γ-inducible protein, and CXCL11/IFN-γ-inducible T-cell α-chemoattractant) within solid and caseous granulomas, and there was only minimal expression in nongranulomatous regions of tissue. The mRNA expression patterns of IFN-γ and tumor necrosis factor alpha were examined in parallel, and the results revealed that cytokine mRNA$^+$ cells were abundant and generally localized to the granulomas. Mycobacterial 16S rRNA expression was also measured by ISH, and the results revealed that there was localization predominantly to the granulomas and that the highest signal intensity was in caseous granulomas. We observed several granulomatous lesions with exceptionally high levels of RNA for mycobacterial 16S rRNA, IFN-γ, and IFN-γ-inducible chemokines, suggesting that the local presence of mycobacteria is partially responsible for the upregulation of IFN-γ-inducible chemokines and recruitment of CXCR3$^+$ cells, which were also abundant in granulomatous lesions. These results suggest that expression of CXCR3 ligands and the subsequent recruitment of CXCR3$^+$ cells are involved in granuloma formation and maintenance.

Tuberculosis is a global public health epidemic; 2 billion people are currently infected with *Mycobacterium tuberculosis*, and 2.2 million deaths occur annually (19). Infection by *M. tuberculosis* typically occurs by inhalation of aerosolized microorganisms into the lungs, which serve as the primary site of infection. A granulomatous lesion develops to contain the bacteria, and this is effective given that 90% of all *M. tuberculosis* infections do not result in active disease (30, 38). *M. tuberculosis* preferentially infects macrophages and appears to be capable of residing in macrophages in a state that is resistant to immune responses. Infected macrophages release cytokines, which increase local inflammation and result in the development of a granulomatous lesion (38).

Granulomas are hallmarks of chronic infectious diseases, such as tuberculosis, brucellosis, and schistosomiasis, and also develop due to the presence of allergens and metals. The granulomatous lesions are generally considered to be the result of chronic antigenic stimulation (10, 36). A tuberculous granuloma is a focal collection of mononuclear cells surrounded by a halo of lymphocytes and additional monocytes (36, 40, 41, 49, 53). The reaction occurs when an infected macrophage becomes encircled by other macrophages and the immune system attempts to wall off the microorganisms to prevent the bacteria from spreading locally and throughout the body. This complex cellular structure can be surrounded by connective tissue, including fibroblasts, collagen fibers, and newly formed vessels (36). A novel morphological characteristic of the granuloma is the presence of epithelioid cells, which occupy the center of each lesion. These epithelioid cells are activated macrophages, which contain increased cytoplasm and disperse chromatin resembling epithelial cells (36). Langhans multinucleated giant cells are also found in granulomas.

M. tuberculosis induces a proinflammatory immune response that is characterized by expression of gamma interferon (IFN-γ), tumor necrosis factor alpha (TNF-α), and interleukin-12 (IL-12) (12, 14, 30–32, 45, 53, 56, 57). Although information has been obtained from bronchoalveolar lavages (BAL) and lung biopsies during advanced disease in humans, only a small number of studies have examined the local cytokine expression patterns associated specifically with granulomas. Examination of BAL cells has indicated that *M. tuberculosis* induces a type 1 polarized cytokine response characterized by IFN-γ expression (4, 8, 50, 55). However, when Fenhalls et al. studied pulmonary granulomas from individuals with active tuberculosis, they found that the expression patterns of IFN-γ relative to those of IL-4 were highly associated with the type of granuloma formed (23). Granulomas with no evidence of caseation expressed either IFN-γ mRNA or IFN-γ mRNA plus IL-4

* Corresponding author. Mailing address: Department of Infectious Diseases and Microbiology, Graduate School of Public Health, University of Pittsburgh, 130 DeSoto St., Pittsburgh, PA 15261. Phone: (412) 648-2341. Fax: (412) 624-4873. E-mail: reinhar@pitt.edu.

mRNA, whereas caseous granulomas expressed little IFN-γ mRNA or IL-4 mRNA (23). These findings suggest that these cytokines play a role in determining granuloma architecture.

The development of a granuloma likely depends on the movement of cells toward the site of inflammation due to expression of chemotactic molecules, although only one study to date has examined local chemokine expression directly in granulomatous tissue sections (24). Proinflammatory chemokines are chemotactic cytokines which play a major role in the recruitment of receptor-bearing cells to sites of inflammation (2, 35). The functions of chemokines include chemotaxis, integrin activation, and degranulation of distinct leukocyte subsets expressing specific chemokine receptors (17). The expression of proinflammatory chemokines is induced by local environmental signals, such as TNF-α or IFN-γ (2, 48). Granulomas induced experimentally with mycobacterial agents lead to the development of type 1 cytokine and chemokine expression profiles (12, 14, 45). IFN-γ induces macrophages and dendritic cells (DC) to produce IFN-γ-inducible CXCR3 ligands, CXCL9/monokine induced by IFN-γ (Mig), CXCL10/IFN-γ-inducible protein with a size of 10 kDa (IP-10), and CXCL11/IFN-γ-inducible T-cell α-chemoattractant (I-TAC), which recruit $CXCR3^+$ cells (52). $CXCR3^+$ cells typically express type 1 cytokines (18) and therefore can potentially induce further upregulation of CXCR3 ligands, leading to chronic type 1 polarized inflammation, which occurs during simian immunodeficiency virus (SIV) infection of rhesus macaques (*Macaca mulatta*) (46).

The local chemokine expression patterns in granulomatous tissues have not been fully examined directly in tissue sections thus far. Experimental *M. tuberculosis* infection in a macaque model induces granuloma formation remarkably similar to that seen in humans infected with this pathogen (11, 34, 62). In this study, we examined the chemokine and cytokine mRNA expression patterns in lung tissues from *M. tuberculosis*-infected cynomolgus macaques (*Macaca fascicularis*) by in situ hybridization (ISH). Our results provide direct evidence that IFN-γ mRNA is present and abundant in the granulomas of infected cynomolgus macaques and that IFN-γ-inducible chemokine mRNAs are upregulated and potentially responsible for the recruitment of $CXCR3^+$ cells that could further skew the immune environment through ongoing IFN-γ production. The abundant expression of IFN-γ-inducible CXCR3 ligands and the inflammatory cytokines IFN-γ and TNF-α directly in solid and caseous granulomas suggests that continual cell recruitment and a state of chronic inflammation likely contribute to the formation and maintenance of tuberculous granulomas.

MATERIALS AND METHODS

Animals and tissue processing. All animal studies were performed under the guidance and with the approval of the University of Pittsburgh Institutional Animal Care and Use Committee. Nine adult cynomolgus macaques were inoculated with a low dose (approximately 25 CFU) of virulent *M. tuberculosis* (Erdman strain) by using a bronchoscope in the lower right lobe, as described elsewhere (11). The infection was allowed to proceed until the macaques reached disease states that spanned a spectrum from no apparent disease to advanced disease. At necropsy, tissues were collected and fixed in 4% paraformaldehyde–1× phosphate-buffered saline for 5 h at 40°C, as previously described (20). After fixation, the tissues were cryoprotected and snap frozen in isopentane cooled on dry ice to −65°C.

Immunohistochemistry. Immunohistochemical staining of 14-μm tissue sections was performed by using cell-type-specific antibodies, including anti-CD3 (clone CD3-12; NovoCastra), anti-CD68 (clone KP1; Dako), anti-CD20 (clone L26; Dako), and anti-CXCR3 (clone 1C6; Pharmingen). Tissue sections were pretreated in 0.01 M sodium citrate (pH 6.0) by microwaving, followed by application of the primary antibody (diluted in 1× phosphate-buffered saline) to the tissues for 1 h in a humid chamber at room temperature. Primary antibodies were detected with the PicTure-Plus detection system (Zymed Laboratories) by using 3,3′-diaminobenzidine as the final substrate.

ISH. Riboprobe synthesis and ISH were performed on 14-μm tissue sections as previously described (15, 20, 46). Cytokine and chemokine mRNAs were detected by ISH by using gene-specific riboprobes. Plasmids containing macaque IFN-γ and TNF-α cDNAs were kindly provided by Francois Villinger (Emory University). Plasmids encoding CXCL9/Mig, CXCL10/IP-10, and CXCL11/I-TAC genes have been described previously (5, 46). The autoradiographic exposure times were 7, 10, and 11 days for chemokine mRNA ISH, cytokine mRNA ISH, and *M. tuberculosis* 16S rRNA ISH, respectively.

Quantitative image capture and analysis. Each granuloma present in lung tissue sections was categorized as a solid or caseous granuloma. ISH signal intensities were measured by quantitative image analysis. Using an RT Slider Spot camera (Diagnostic Instruments, Inc.), we captured images of all granulomas with a ×4 objective lens. The MetaView software package (Universal Imaging Corp.) was used to measure the surface area covered by autoradiographic silver grains, as well as the total surface area of the granuloma. After color separation, the green channel was converted to pseudocolor, and the image was thresholded to measure the surface area covered by silver grains.

***M. tuberculosis* 16S rRNA subcloning and sequencing.** The 16S ribosomal DNA from *M. tuberculosis* strain H37Rv was amplified by PCR by using sequence-specific forward primer 5′-GGCGTGCTTAACACATGCAA-3′ and reverse primer 5′-CGCTCACAGTTAAGCCGT-3′, as previously described (43). The amplified product (550 bp) was subcloned into pGEMT, and the DNA was sequenced, which revealed 100% homology to 16S rRNA genes of both the H37Rv and CDC1551 strains of *M. tuberculosis* (data not shown).

RESULTS

Classic granulomatous lesions arise in macaque pulmonary tissues. To address key issues regarding granuloma formation and maintenance in a nonhuman primate model, cynomolgus macaques were inoculated intrabronchially with a low dose of virulent *M. tuberculosis* (Erdman strain). All nine animals examined in this study were successfully infected, as demonstrated by a tuberculin skin test, by the peripheral blood mononuclear cell lymphoproliferative response to mycobacterial antigens, by positive bacterial cultures obtained from BAL, and by radiographic observations. Detailed clinicopathological and bacteriological findings have been presented separately (11). The animals varied in the rate and extent of disease progression, but all of the animals had macroscopic (gross) lesions in the lung tissues at necropsy. They were classified as exhibiting minimal or moderate disease or advanced disease based on their clinical condition and on gross and microscopic pathological findings. The pulmonary granulomas detected in the tissue sections varied in size and structure (Table 1). We examined more than 300 granulomas in seven of the nine animals, and 93% of the granulomas were observed in animals with advanced disease (Table 1). The surface areas of the granulomas in 14-μm tissue sections ranged from 1.5×10^4 to 5.5×10^6 μm^2, and approximately two-thirds of the granulomas were caseous. If macaque M15300, which harbored the majority of the granulomas examined, was removed from the summary, the mean surface areas for solid and caseous granulomas were 1.4×10^5 and 7.1×10^5 μm^2, respectively, and 37% of the granulomas were caseous. Caseous granulomas were present in all of the animals with granulomas, but the majority of these granulomas were observed in the macaques with advanced disease. Solid granulomas were present more

TABLE 1. Animals and clinicopathological findings

Animal	Duration of infection (weeks)	Radiographic results[a]	Disease course	Granulomas			
				Total no.[e]	No. of solid granulomas	No. of necrotic granulomas	Size (μm^2)[f]
M7100	9[b]	+	Moderate disease	2	0	2	424,136–1,820,000
M15300	10[c]	+++	Advanced disease	233	56	177	16,836–5,486,090
M15000	16[b]	++	Moderate disease	13	12	1	20,185–996,507
M14600	17[b]	−	No disease[d]	0			
M15100	17[b]	+	Moderate disease	7	6	1	33,606–1,020,000
M11301	32[c]	+++	Advanced disease	15	9	6	40,992–1,250,000
M11201	37[c]	+++	Advanced disease	24	12	12	28,620–2,327,970
M7200	41[c]	+++	Advanced disease	7	4	3	14,882–2,060,000
M15200	64[b]	−	Minimal disease	0			

[a] Radiographic results at necropsy. M14600 was the only macaque that did not have a positive radiographic result. However, viable *M. tuberculosis* bacilli were cultured from lung homogenates at necropsy. Scoring of − to +++ was based on the extent of involvement as described previously (11).
[b] Sacrificed at a scheduled time.
[c] Sacrificed due to extreme clinical symptoms.
[d] Only a few macroscopic granulomas were observed at necropsy.
[e] Number of granulomas examined in tissues.
[f] Surface area in 14-μm tissue sections.

frequently than caseous granulomas in animals with minimal or moderate disease. However, animals with advanced disease harbored more granulomas, and therefore, the majority of the solid granulomas were observed in these macaques.

The cellular compositions of the granulomatous structures were examined by immunohistochemical (IHC) staining of formalin-fixed, cryopreserved tissue sections. Both solid and caseous granulomas were predominantly comprised of macrophages ($CD68^+$) and lymphocytes (Fig. 1). The lymphocytes were mainly T lymphocytes ($CD3^+$), but B lymphocytes ($CD20^+$) were also detected in the granulomatous lesions as a mixed population of diffusely and intensely staining cells (Fig. 1G and H). Regardless of the disease state, the compositions of the numerous granulomas were similar in all macaques. $CD68^+$ cells (Fig. 1C and D) were more abundant than the other cell types examined, and the staining pattern was distributed throughout the cellular portions of the lesions. The T lymphocytes ($CD3^+$) (Fig. 1E and F) were dispersed throughout the cellular portions of the granulomatous lesions, whereas the rare B lymphocytes ($CD20^+$) (Fig. 1G and H) were not in a particular location but were localized in peripheral focal collections in caseous granulomas. The $CD4^+/CD8^+$ ratio of T lymphocytes for a small number of disaggregated granulomas from five animals ranged from 0.37 to 1.11 (mean, 0.68). Together, these data indicate that cynomolgus macaques inoculated intratracheally with a low dose of virulent *M. tuberculosis* develop classic granulomas.

Abundant expression of IFN-γ-inducible CXCR3 ligands in granulomatous lesions. Chemokines likely play multiple roles in *M. tuberculosis*-associated granuloma formation and maintenance, including shaping of the local immune environment. Since IFN-γ is a cytokine that is critical for host resistance to *M. tuberculosis* disease progression in mice and humans (16, 25, 29, 39), we determined the patterns and levels of expression of mRNAs encoding the IFN-γ-inducible chemokines CXCL9/Mig, CXCL10/IP-10, and CXCL11/I-TAC directly in lung tissues from experimentally infected macaques. This approach can reveal changes in mRNA expression levels that might not be as evident if RNAs from homogenized tissues are used in population analyses. ISH of these CXCR3 ligand mRNAs revealed extremely abundant expression within the granulomatous lesions; the highest signal was observed for CXCL9/Mig and the lowest signal was observed for CXCL11/I-TAC in both solid and caseous granulomas (Fig. 2). In contrast, nongranulomatous regions of lung tissue and lung tissue from *M. tuberculosis*-naïve control macaques rarely exhibited appreciable expression of any CXCR3 ligand mRNA (Fig. 2) (data not shown). Solid granulomas had intense ISH signals concentrated only in the central portions of the granulomas, whereas caseous granulomas had intense ISH signals concentrated in the cellular portions of the granulomas surrounding the acellular centers (Fig. 2).

To measure mRNA expression, we performed quantitative image analysis of the tissue sections using the MetaView software package. We measured the total surface area of each granuloma, as well as the proportion of the cellular surface area covered by autoradiographic silver grains. Acellular, necrotic regions were excluded from the calculations. As expected, the amount of thresholded surface area attributed to silver grains increased as the total surface area of the granuloma increased for both solid and caseous granulomas (data not shown). We then determined the percentage of cellular surface area covered by ISH signals (Fig. 3). The percentage of thresholded surface area measured for cellular portions of granulomas for the CXCL9/Mig ISH signal was the highest percentage for the three CXCR3 ligand mRNAs, and the mean percentages of thresholded area were 48 and 51% for solid and caseous granulomas, respectively (Table 2). The mean percentages of thresholded surface area for CXCL9/Mig, CXCL10/IP-10, and CXCL11/I-TAC in the granulomas from animals with advanced disease were approximately twofold higher than the mean percentages in the granulomas from animals with minimal or moderate disease (Fig. 3 and Table 2). In summary, IFN-γ-inducible chemokines were dramatically upregulated in macaque pulmonary granulomatous lesions compared to the levels in nongranulomatous tissue and naïve controls.

The high levels of expression of CXCR3 ligands would be expected to lead to recruitment of $CXCR3^+$ cells to the local environment. To identify $CXCR3^+$ cells, we performed IHC

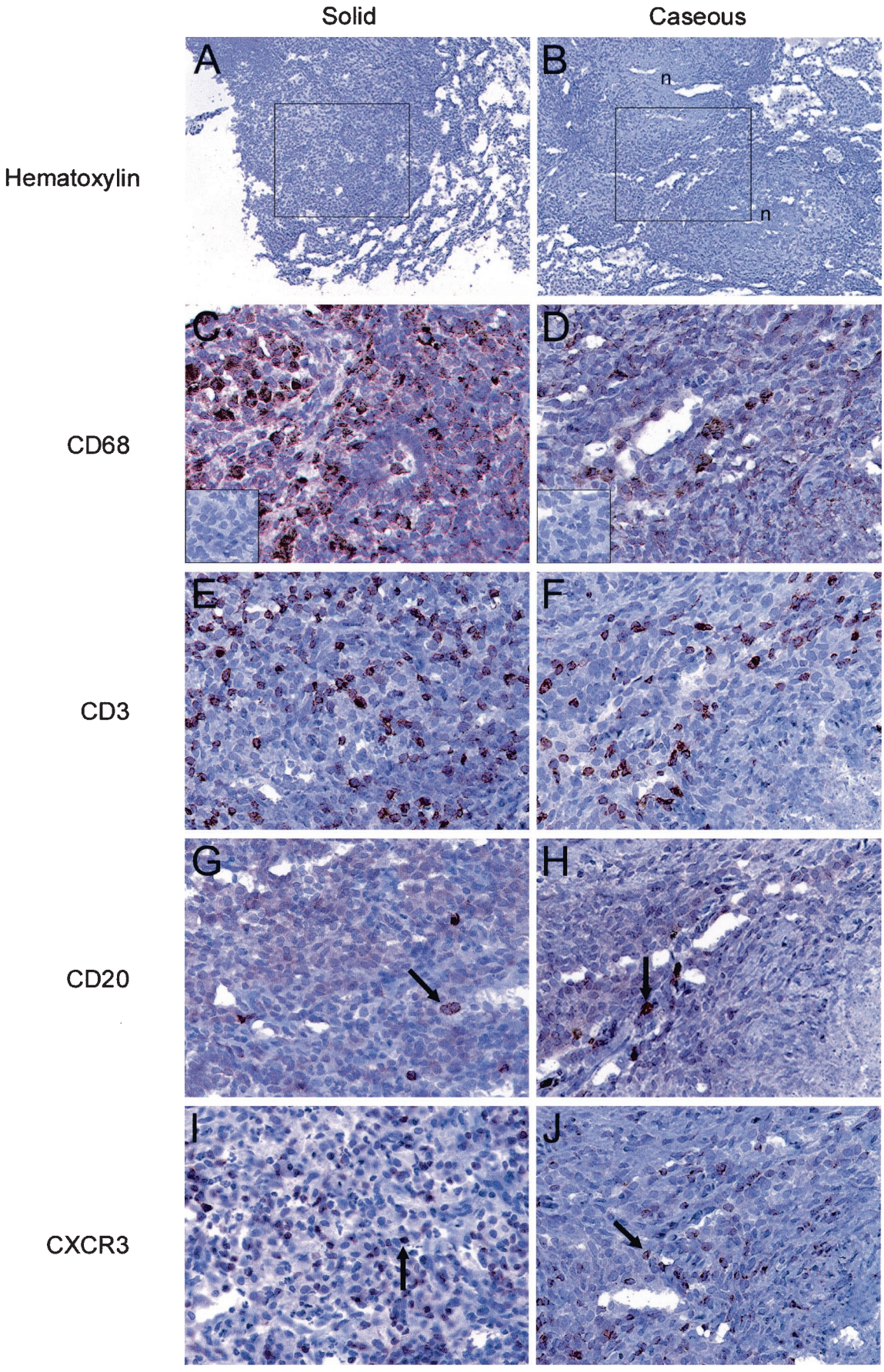
Solid
Caseous
Hematoxylin
CD68
CD3
CD20
CXCR3
A
B
n
n
C
D
E
F
G
H
I
J

TABLE 2. Quantitation of chemokine, cytokine, and mycobacterial RNA expression in granulomatous lesions of cynomolgus macaques experimentally infected with *M. tuberculosis*

Lesions	Disease severity	Animal	No. of granulomas	Granuloma size (μm^2)[a]	No. of mycobacterial rRNA collections[b]	No. of IFN-γ mRNA$^+$ cells[c]	No. of TNF-α mRNA$^+$ cells[c]	CXCL9/ Mig ISH signal (%)[d]	CXCL10/ IP-10 ISH signal (%)[d]	CXCL11/ I-TAC ISH signal (%)[d]
Solid	Minimal or moderate	M15000	12	184,882	0.9	38.2	31.2	23.54	35.89	8.47
		M15100	6	157,386	0.0	6.5	2.5	9.54	6.83	1.56
		Avg		175,717	0.8	27.0	21.1	18.29	17.58	6.17
	Advanced	M7200	4	189,597	2.0	46.0	NA[e]	26.96	19.37	31.07
		M11201	12	135,894	NA	2.8	3.1	55.68	43.10	6.82
		M11301	9	131,056	1.4	39.4	11.2	49.53	42.59	27.11
		M15300	56	337,018	3.9	20.6	14.1	57.15	28.37	15.87
		Avg		277,057	3.5	23.1	11.6	55.02	32.08	17.15
	All[f]			258,631	2.8	24.1 (0–156)	14.0 (0–130)	48.03 (1.33–84.22)	29.15 (0.16–90.53)	14.48 (0.08–75.44)
Caseous	Minimal or moderate	M7100	2	1,122,068	NA	114.0	42.0	40.23	23.48	10.01
		M15000	1	996,507	0.0	47.0	NA	30.60	22.60	0.26
		M15100	1	1,020,000	NA	20.0	10.0	16.86	8.17	1.99
		Avg		1,065,161	0.0	60.3	26.0	29.23	18.09	5.57
	Advanced	M7200	3	875,262	4.3	92.3	NA	32.61	27.14	22.95
		M11201	12	591,442	NA	39.6	13.0	60.11	41.27	12.88
		M11301	6	634,611	246.0	112.8	28.8	51.93	44.15	22.16
		M15300	177	678,735	4.1	49.1	28.0	51.32	32.75	11.52
		Avg		675,010	45.17	51.8	26.9	51.58	33.53	12.00
	All[f]			682,892	45.0	51.9 (1–238)	26.9 (2–135)	51.19 (14.14–99.38)	33.25 (0.35–74.44)	11.83 (0.26–40.16)

[a] Average surface area of granulomas per 14-μm section.
[b] Average number of mycobacterial 16S rRNA focal collections per 14-μm section of granuloma.
[c] Average number of mRNA$^+$ cells per 14-μm section of granuloma.
[d] Average percentage of cellular surface area comprised of autoradiographic silver grains.
[e] NA, not available.
[f] Average (range) for all lesions in each group.

staining with an anti-CXCR3 monoclonal antibody (Fig. 1I and J). CXCR3$^+$ cells were more abundant in granulomatous regions than in nongranulomatous regions of macaque lung tissues. The CXCR3$^+$ cells were not concentrated only in specific areas of the granulomatous lesions but were generally well localized with expression of the CXCR3 ligand mRNAs. The increased abundance of these receptor-bearing cells in the granulomatous lesions was consistent with increases in CXCR3 expression in BAL cells obtained from the same macaques (data not shown)

Expression of IFN-γ and TNF-α mRNAs is elevated in granulomatous lesions. Previous studies have shown that IFN-γ plays a protective role in the host response to *M. tuberculosis*, that TNF-α is important in granuloma formation and maintenance (6, 9, 13, 48), and that both cytokines can induce expression of subsets of chemokines (2, 48). Therefore, we examined the patterns and levels of expression of the mRNAs of these cytokines in *M. tuberculosis*-induced granulomatous lesions in cynomolgus macaques. TNF-α and IFN-γ mRNA$^+$ cells were abundant in the granulomatous lesions of these macaques (Fig. 2I to L) but were extremely rare in nongranulomatous regions of lung tissue sections. These TNF-α and IFN-γ mRNA$^+$ cells were found in the cellular regions of granulomas and colocalized with the IFN-γ-inducible chemokine ISH signal (Fig. 2C to H). In contrast, no IL-4 mRNA$^+$ cells were observed in any of the same tissue sections (data not shown). As a measure of local cytokine mRNA expression, we manually counted the cytokine mRNA$^+$ cells in each granuloma. An ISH signal for IFN-γ mRNA was present as a dense focal collection of silver grains (Fig. 2I and J), whereas an ISH signal for TNF-α mRNA was present as networks of more diffuse signal (Fig. 2K and L). The number of IFN-γ mRNA$^+$ cells per 14-μm granuloma section was greater than the number of TNF-α mRNA$^+$ cells in both groups of animals (Fig. 3B and Table 2), and caseous

FIG. 1. Structures and cellular compositions of lung granulomas of cynomolgus macaques experimentally infected with *M. tuberculosis*. Each granuloma in lung tissue sections was categorized as solid (e.g., animal M11201) (A, C, E, G, and I) or caseous (e.g., animal M11301) (B, D, F, H, and J). The boxes in panels A and B indicate the regions of the granulomas in subjacent sections which are shown in panels C to J, and the necrotic portions of the granulomas are also indicated (n). Specific cell types were identified by IHC staining by using antibodies directed against CD68 (C and D), CD3 (E and F), CD20 (arrows) (G and H), and CXCR3 (arrows) (I and J). CXCR3$^+$ cells were also detected as an indirect measure of the recruitment of CXCR3$^+$ cells to the granuloma (I and J). The necrotic portions of the granulomas are in the top left and bottom right corners of the micrographs in panels D, F, H, and J. A parallel analysis with isotype control antibodies yielded no IHC signal (insets in panels C and D). Original magnifications, ×100 (A and B) and ×200 (C to J).

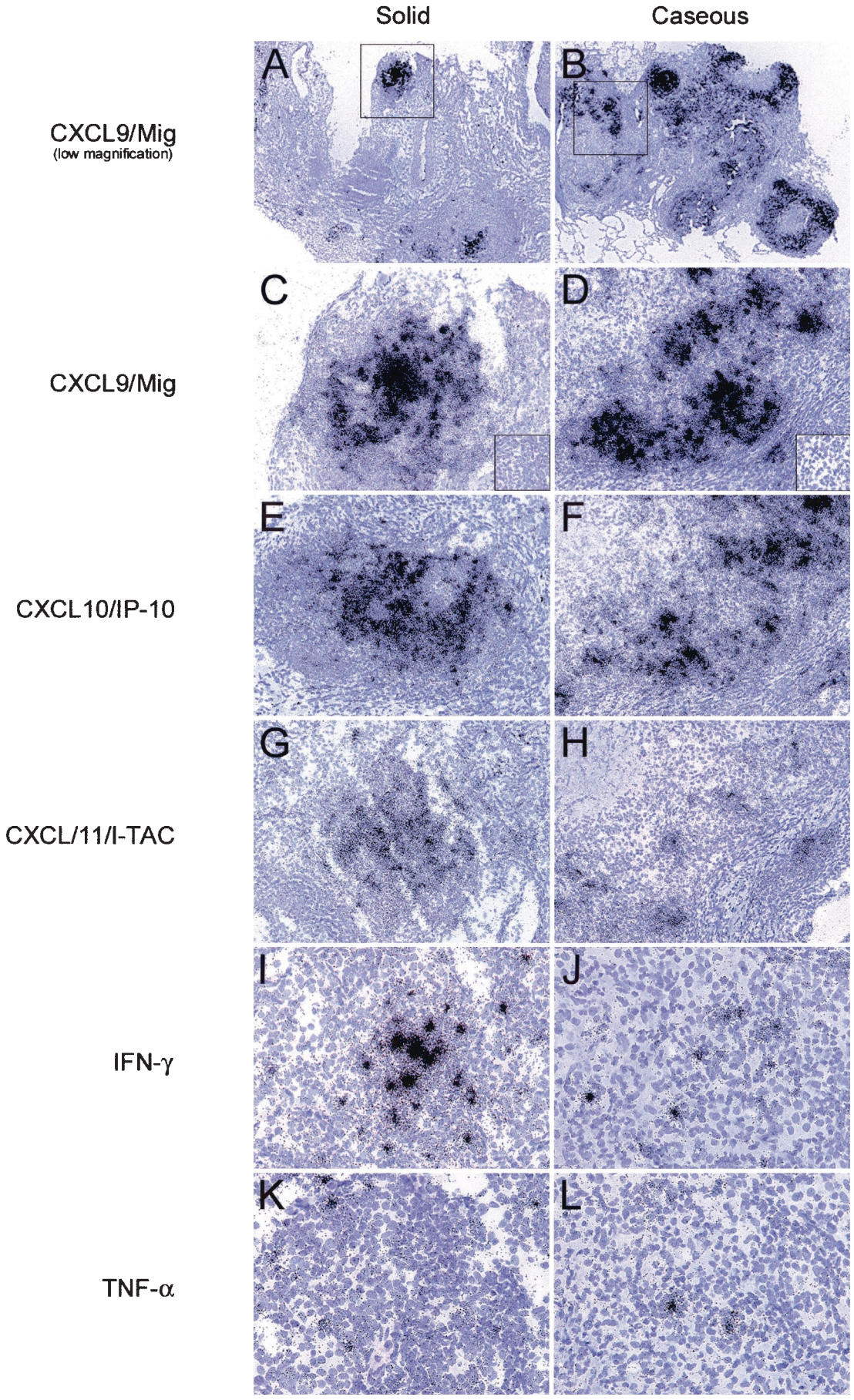
Solid
Caseous
CXCL9/Mig
(low magnification)
CXCL9/Mig
CXCL10/IP-10
CXCL/11/I-TAC
IFN-γ
TNF-α
A
B
C
D
E
F
G
H
I
J
K
L

granulomas harbored higher numbers of IFN-γ mRNA$^+$ cells per granuloma than solid granulomas harbored (Fig. 3B and Table 2). The average numbers of IFN-γ mRNA$^+$ cells were 24 and 52 mRNA$^+$ cells per 14-μm section of granuloma for solid and caseous granulomas, respectively (Table 2), whereas the average numbers of TNF-α mRNA$^+$ cells were 14 and 27 mRNA$^+$ cells per section of granuloma for solid and caseous granulomas, respectively. However, the mean values in Table 2 indicate that the numbers of IFN-γ mRNA$^+$ cells present in the cellular regions of granulomas were roughly proportional to granuloma size.

Detection and quantitation of *M. tuberculosis* 16S rRNA in pulmonary granulomatous lesions. The high levels of chemokine and cytokine mRNA expression which we observed in granulomatous lesions might have been associated with high numbers of local mycobacteria or mycobacterial products. To address this possibility, we performed ISH using a riboprobe specific for mycobacterial 16S rRNA. ISH with this riboprobe readily allowed detection of the mycobacterial 16S rRNA in lung tissue sections of cynomolgus macaques (Fig. 4). No specific ISH signal was detected in the corresponding sense control probe experiments (Fig. 4E, inset). The ISH signal observed was typically a compact collection of silver grains or, more rarely, a more diffuse collection of silver grains scattered over an entire lung cell. We based our enumeration of the mycobacterial 16S rRNA$^+$ focal collections on the assumption that a focus represented either a single bacterium or a collection of bacteria that could not be individually distinguished. Although mycobacterial 16S rRNA$^+$ foci were detected in both solid (Fig. 4A) and caseous (Fig. 4B) granulomas, they were more abundant in the caseous granulomas, and they were also more abundant in the macaques with advanced disease than in the macaques with minimal or moderate disease. The mycobacterial 16S rRNA$^+$ focal collections were observed in both the cellular regions and the central caseating portions of granulomas. Frequently, 16S rRNA$^+$ focal collections were in close proximity to each other in cellular regions of granulomas, but the greatest ISH signals were observed in the acellular centers of caseous granulomas. In animal M11301 with advanced disease, 1,820 16S rRNA$^+$ foci were detected in a single 14-μm section of an exceptional granuloma (Fig. 4C). If we assumed that this entire granuloma was spherical and that the tissue section represented the largest diameter of the granuloma, the entire granuloma (2.5×10^{10} μm^3) was estimated to harbor a minimum of 303,394 mycobacteria. The IFN-γ mRNA ISH signal obtained in a subjacent section of the same granuloma was extremely high (Fig. 4D), as were the intense ISH signals for TNF-α and CXCR3 ligand mRNAs (data not shown).

In another animal with advanced disease (animal M15300), we observed a cavitating lesion (Fig. 4E and F). This lesion, which protruded into an airway, had high numbers of mycobacterial 16S rRNA$^+$ focal collections in the protruding region (Fig. 4E). The local expression of IFN-γ mRNA was also exceptionally abundant (Fig. 4F), and the ISH signal colocalized with the 16S rRNA$^+$ foci. CXCR3 ligand mRNA expression was similarly abundant in this cavitating lesion (data not shown).

DISCUSSION

In this study we examined local chemokine and cytokine mRNA expression and the local mycobacterial burden in pulmonary granulomatous lesions resulting from intrabronchial infection of cynomolgus macaques with a low dose of virulent *M. tuberculosis*. This was one of the first studies of chemokine expression directly in granulomatous tissue sections. We found abundant expression of mRNAs encoding the proinflammatory cytokines IFN-γ and TNF-α, as well as IFN-γ-inducible CXCR3 ligands, within all granulomas regardless of size or structure. The general absence of cells expressing these mRNAs in nongranulomatous regions of lung tissues suggests that they play a local role in granuloma formation and maintenance. Based on these findings we propose a model for *M. tuberculosis*-initiated, IFN-γ-driven chronic inflammation in pulmonary granulomas that is similar to a model for the events occurring in lymphoid tissues of SIV-infected rhesus macaques (46).

Cynomolgus macaques are susceptible to *M. tuberculosis* infection and develop disease that is clinically, immunologically, and pathologically similar to human disease (11, 34, 62). Interestingly, approximately 40% of cynomolgus macaques infected with a low dose of *M. tuberculosis* were able to contain the infection in a subclinical state during the period of study. This subclinical state resembles clinical latency in humans (11, 62) and indicates that cynomolgus macaques are an appropriate animal model for latency (11, 62) and reactivation (11) during *M. tuberculosis* infection. Although the proportion of cynomolgus macaques that develop active disease is higher, it is similar to the outcome of infection in humans, in which only 10% of individuals infected with *M. tuberculosis* develop overt disease. At the tissue level, *M. tuberculosis*-induced granulomas in cynomolgus macaques are structurally similar to granulomas that develop in humans.

We demonstrated by direct analysis of tissue sections using ISH that there are high levels of expression of IFN-γ-inducible chemokine mRNAs and increased numbers of IFN-γ and TNF-α mRNA$^+$ cells in pulmonary granulomas. CXCR3$^+$ cells, which are predominantly activated T and B lymphocytes and NK cells (42, 51, 52, 54), are likely recruited to the local

FIG. 2. ISH detection of IFN-γ-inducible chemokine and cytokine mRNAs in granulomatous lung tissues from *M. tuberculosis*-infected cynomolgus macaques. ISH was performed with lung tissue sections by using IFN-γ-inducible chemokine- and cytokine-specific riboprobes, and representative fields from subjacent sections are shown. Low-magnification micrographs of the ISH for CXCL9/Mig highlight the granulomatous tissue in panels A and B, and the boxes indicate the granulomatous regions that are shown in panels C to L. ISH was performed for CXCL9/Mig (C and D), CXCL10/IP-10 (E and F), and CXCL11/I-TAC (G and H) mRNAs in solid (C, E, and G) and caseous (D, F, and H) granulomas. IFN-γ (I and J) and TNF-α (K and L) mRNAs were detected by ISH in solid (I and K) and caseous (J and L) granulomatous lesions. The necrotic portion of the granuloma is in the top left corner of the micrographs in panels D, F, H, J, and L. Parallel hybridizations with control sense riboprobes resulted in no autoradiographic signal (insets in panels C and D). Original magnifications, ×20 (A and B), ×100 (C to H), and ×200 (I to L).

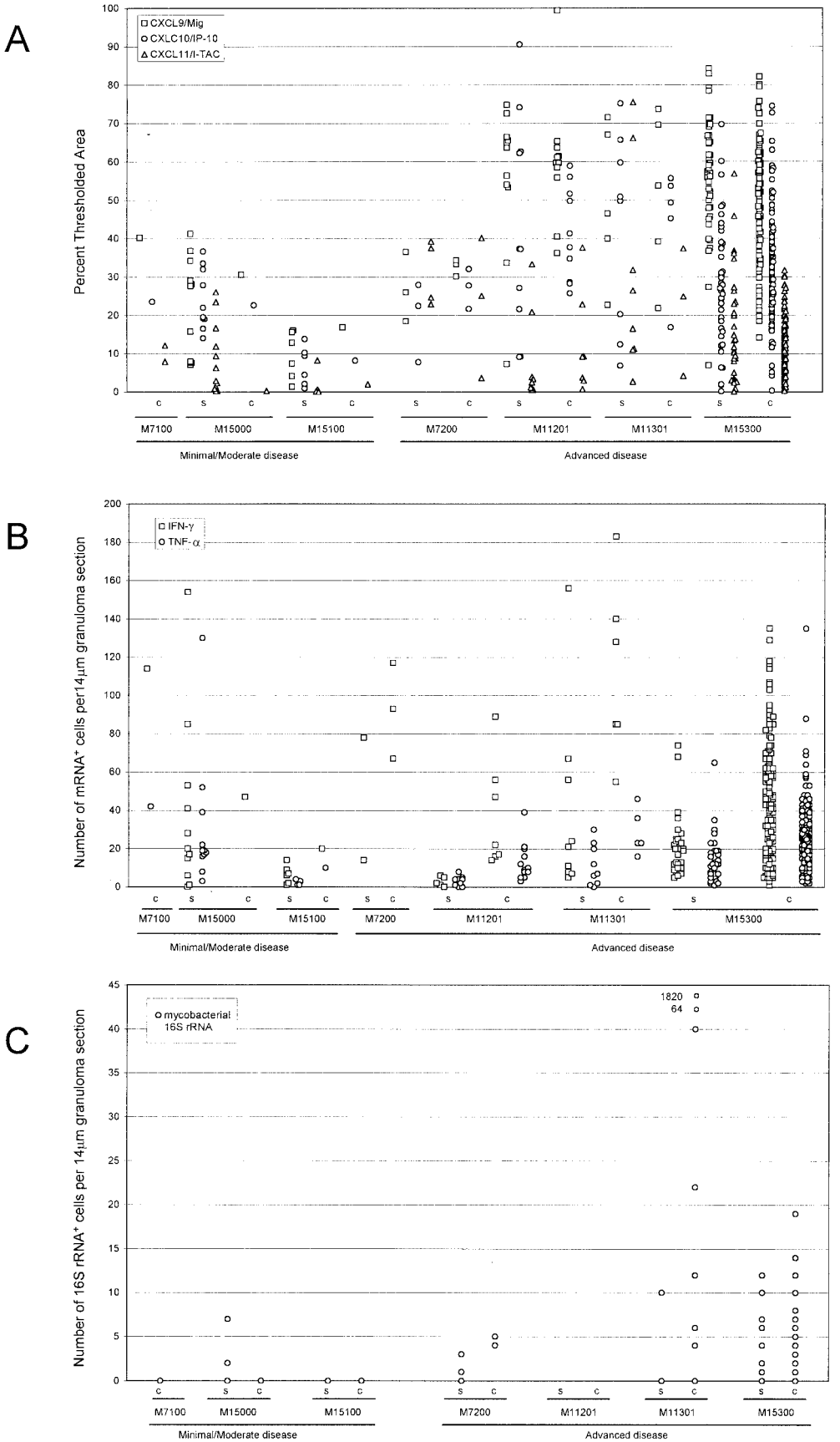

FIG. 3. Quantitative image analysis of ISH signals for IFN-γ-inducible chemokine and cytokine mRNAs and mycobacterial 16S rRNA in granulomatous lesions. Chemokine-specific ISH, cytokine-specific ISH, and mycobacterium-specific ISH were performed with granulomatous lung tissues from experimentally infected macaques. For quantitation of the chemokine mRNA ISH signal, a digital image of each granuloma was

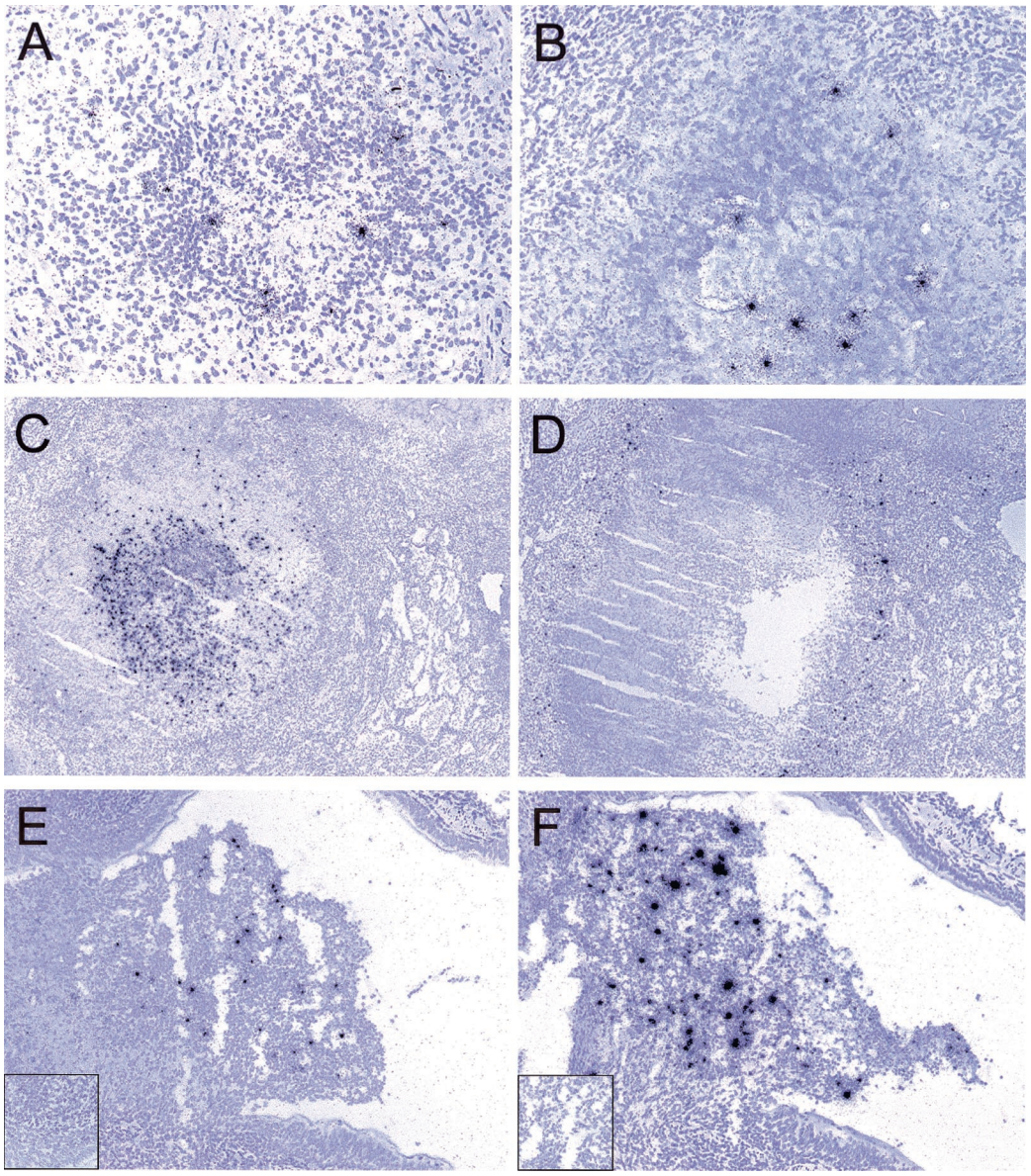

FIG. 4. ISH detection of mycobacterial 16S rRNA and IFN-γ mRNA in granulomas in experimentally infected cynomolgus macaques. ISH was performed with lung tissues by using riboprobes specific for the mycobacterial 16S rRNA and IFN-γ RNAs, and representative fields are shown. Mycobacterial 16S rRNA was detected in tissues with solid (e.g., animal M15000) (A) and caseous (e.g., animal M15300) (B) granulomas in animals with moderate disease (A) and advanced disease (B). Necrotic granulomas with abundant mycobacterial 16S rRNA (animal M11301) (C) and IFN-γ mRNA (animal M11301) (D) ISH signals are also shown, as are cavitating lesions with abundant 16S rRNA (animal M15300) (E) and IFN-γ mRNA (animal M15300) (F) ISH signals. Parallel hybridizations with control sense riboprobes provided no autoradiographic signal (insets in panels E and F). Original magnifications, ×20 (E and F), ×100 (A, C, and D), ×200 (B).

environment. Our detection of abundant $CXCR3^+$ cells in pulmonary granulomas provides evidence that this recruitment occurs. Although not examined here, local proliferation and apoptosis also likely contribute to accumulation and loss of cells, respectively, and affect overall granuloma size and structure.

Previous studies of chemokine expression during *M. tuberculosis* infection included in vivo murine studies and ex vivo and limited tissue-based human studies. Mice infected by the aerosol route exhibited increases in CCL3/MIP-1α, CXCL2/MIP-2, CXCL10/IP-10, and CCL2/MCP-1 expression in lungs (47). In addition, granulomas elicited in mice by purified pro-

captured. The proportion of cellular surface area covered by silver grains was determined by using the threshold and measure tools of the MetaView software package (A). The numbers of IFN-γ and TNF-α $mRNA^+$ cells per 14-μm section of granuloma were determined for each solid and caseous granuloma (B). To measure the local mycobacterial load, ISH for mycobacterial 16S rRNA was performed, and the numbers of mycobacterial 16S $rRNA^+$ cells and focal collections were determined for 14-μm sections of each solid and caseous granuloma (C). Each data point represents the value obtained for an individual granuloma. c, caseous; s, solid.

tein derivative-coated beads had a polarized type 1 immune response with increased levels of expression of CXCL2/MIP-2, CXCL5/LIX, CXCL10/IP-10, and CXCL9/Mig (14, 45). In these studies, neutralization of IFN-γ with antibodies greatly reduced the expression of CXCL9/Mig and CXCL10/IP-10. Human studies of patient-derived BAL or alveolar and peripheral macrophages revealed increased expression of CXCL8/IL-8, CCL5/RANTES, CCL3/MIP-1α, CCL2/MCP-1, and CXCL10/IP-10 (24, 53). The one other ISH and IHC report of chemokine expression in human tuberculous granulomas demonstrated that there was localized expression of CXCL10/IP-10, CXCL8/IL-8, and CCL2/MCP-1 within granulomas (24).

The strategy which we have used for detection of cells producing proinflammatory chemokines and cytokines is targeted toward mRNA expressed by the producing cell. This approach reveals the locations and numbers of cells that produce these immunomodulatory proteins, but it does not indicate the locations or amounts of actual proteins. Although this is a limitation of our study, the detection of chemokine and cytokine proteins is complicated by the diffusion of proteins that occurs after release into the extracellular milieu. The detection of different proteins by IHC is also complicated by the unique physiochemical properties of each antigen-antibody pair compared to the properties of RNA-RNA hybrids, which generally have the same physiochemical properties. Our ISH strategy has the additional advantage that it can reveal focal changes in mRNA expression that might not be detected by population analyses of extracted tissue RNAs due to dilution.

Previous in situ studies of human tuberculous granulomas revealed local production of TNF-α and IFN-γ mRNAs in all granulomatous lesions, but only a fraction of these lesions expressed IL-4 mRNA (23). Our data are consistent with these findings in that IFN-γ mRNA was much more abundant than IL-4 mRNA, but they differ in that we did not detect any IL-4 mRNA by our ISH assay, as also observed by other workers with human granulomas (3). Limited expression of both IFN-γ and IL-4 mRNAs has been suggested to be associated with progression of granulomas to a necrotic state (23). However, we observed an association between the numbers of local IFN-γ and TNF-α mRNA$^+$ cells and the sizes (and necrotic states) of pulmonary granulomas. The reasons for the differences between our findings and those of other workers (23) are not clear but could include differences with respect to (i) the host species studied, (ii) the disease and treatment status of the study subjects, (iii) the tissue-processing protocols, and/or (iv) the ISH probe and detection strategies.

Based on our finding that there was abundant expression of CXCR3 ligands, IFN-γ, and TNF-α in pulmonary granulomatous lesions, we propose a model for the contributions of these molecules to the chronic inflammation that results in granuloma formation and maintenance, which is similar to a model previously proposed for chronic inflammation in SIV-infected lymphoid tissues (46). First, infection of alveolar macrophages or DC leads to induction of proinflammatory cytokines and chemokines (for example, by interaction of mycobacterial antigen with Toll-like receptors [TLRs]). Additional cells are therefore recruited to the local environment. Immune responses specific to *M. tuberculosis* develop following the trafficking of pulmonary DC to draining lymph nodes, which results in the trafficking of type 1 CD4$^+$ and CD8$^+$ T lymphocytes to the site of *M. tuberculosis* infection, and these cells produce IFN-γ. IFN-γ function is enhanced in the presence of TNF-α, which is well documented as an important cytokine in the immune response to *M. tuberculosis* and in granuloma formation (6, 9, 13, 48). Both local production of IFN-γ and TLR stimulation induce the expression of CXCR3 ligands and thus recruit CXCR3$^+$ T lymphocytes and NK cells to the site of *M. tuberculosis* infection. CXCR3 ligands contribute to further polarization of the local environment because they augment the ability of IFN-γ to induce additional CXCR3 ligand production and lead to a type 1 outcome following stimulation of T lymphocytes with polyclonal activators or specific antigens (28). In this model, the collective outcome is the establishment and maintenance of a positive feedback loop in which local IFN-γ production leads to the ongoing recruitment of additional IFN-γ-producing cells. Also, this suggests that IFN-γ has a role in granuloma formation and maintenance beyond induction of an antimicrobial state in infected cells. Thus, there are common themes in *M. tuberculosis* and SIV infections of macaques that, if recapitulated in humans infected with both organisms, might contribute to a significantly poorer prognosis than the prognosis for individuals infected with either pathogen alone.

In addition to effects of antigen-specific type 1 immune responses, *M. tuberculosis* bacilli or mycobacterial components also have direct effects on local cytokine and chemokine expression profiles in and near pulmonary granulomas. In vitro analyses have demonstrated that mycobacterial cell wall components induce expression of proinflammatory cytokines via TLR-2 and TLR-4 (37, 58). Although alveolar macrophages are initially involved in the uptake of *M. tuberculosis*, DC and monocyte-derived interstitial macrophages also phagocytose and process *M. tuberculosis* (59). Interestingly, Lande et al. recently demonstrated that *M. tuberculosis* infection of DC leads to induction of CXCL9/Mig and CXCL10/IP-10, the latter in an IFN-αβ-dependent fashion (33).

In this model we have not included other complex factors, such as complex multichemokine gradients that lead to simultaneous synergistic or antagonistic signals on cells (26). In addition, there are likely to be negative regulatory activities that occur at the same time. A candidate for such regulation is the lymphocyte cell surface protein CD26 (also known as dipeptidylpeptidase IV), which catalyzes the removal of N-terminal dipeptides from suitable substrates containing a penultimate proline or alanine (60). Cleavage by CD26 differentially affects the activity of specific chemokines, rendering some chemokines inactive and others more potent (60). CD26 proteolytically processes all three CXCR3 ligands and converts them to antagonists of CXCR3-mediated chemotaxis (44). Determination of the roles played by such complex factors in granuloma formation and maintenance requires further analysis.

To determine whether the immunologic events that occur in granulomatous lesions are due to the abundance of local *M. tuberculosis* bacilli or products, we developed an ISH strategy for detection of mycobacterial 16S rRNA directly in tissue sections. One frequently used strategy for in situ detection of *M. tuberculosis* is acid-fast staining. However, the sensitivity of this procedure is reduced by the common treatment of tissues with formalin and xylene (27). Overall, we found a relatively

low number of foci hybridizing to the mycobacterial 16S rRNA probe in most animals, although two animals with advanced disease had much higher levels of signal. Most of the mycobacterial 16S rRNA ISH signal was localized to the necrotic portions of the granulomas, although some signal was localized to the cellular regions of caseous and solid granulomas. Our probe for detection of *M. tuberculosis* does not discriminate between viable and nonviable organisms or between metabolically active and inactive states of the bacillus, but it detects an RNA target that is stable and abundant (1, 7, 61). This might explain the different localization of the *M. tuberculosis* ISH signal in our study compared to the localization in the studies of Fenhalls et al. (21, 22), in which the ISH signal was localized to cells in the cellular and surrounding regions of the granulomas. Once they reach a certain size or have a certain fluidic composition, the necrotic centers of caseous granulomas might provide a hospitable environment for the organism. Further studies with additional probes and tuberculosis cases and stages are needed to fully understand the importance of the numbers and states of mycobacterial organisms for granuloma formation and maintenance.

In summary, through examination of over 300 *M. tuberculosis*-induced pulmonary granulomas in experimentally infected cynomolgus macaques, we demonstrated that there was abundant IFN-γ-inducible chemokine and IFN-γ and TNF-α cytokine mRNA expression within the granulomas. The abundant staining of $CXCR3^+$ cells in the same microenvironments is consistent with recruitment of these cells to the granulomas. These findings, as well as our findings of colocalized *M. tuberculosis* 16S rRNA in the pulmonary granulomas, suggest that the nature of the type 1 immune response and the direct action of mycobacterial components together lead to the establishment of chronic inflammation. There must be a complex balance among the inflammatory responses, antigen-specific responses, and negative regulatory mechanisms that determines the extent to which a granuloma contains the bacillus or develops into a structure that allows the organism to multiply and spread within and among hosts. Additional definition of the contributions of IFN-γ-inducible and other chemokines to these processes should elucidate mechanisms by which granulomas successfully limit or eliminate *M. tuberculosis* bacilli. These data should be important for developing additional strategies to combat morbidity and mortality caused by *M. tuberculosis*.

ACKNOWLEDGMENTS

We thank Beth A. Fallert and Kelly Whelton for expert technical assistance, Denise Croix and Saverio Capuano III for their advice and for care of the animals, Santosh Pawar for flow cytometric information on granuloma T-lymphocyte populations, and Francois Villinger for plasmids containing macaque cytokine cDNAs.

This study was supported by NIH grant AI-47485 to J.L.F.

REFERENCES

1. **Alberts, B., D. Bray, J. Lewis, M. Raff, K. Roberts, and J. D. Watson.** 1989. Control of gene expression, p. 595. *In* Molecular biology of the cell. Garland Publishing, Inc., New York, N.Y.
2. **Baggiolini, M.** 1998. Chemokines and leukocyte traffic. Nature **392:**565–568.
3. **Barnes, P. F., S. Lu, J. S. Abrams, E. Wang, M. Yamamura, and R. L. Modlin.** 1993. Cytokine production at the site of disease in human tuberculosis. Infect. Immun. **61:**3482–3489.
4. **Barry, S. M., M. C. Lipman, B. Bannister, M. A. Johnson, and G. Janossy.** 2003. Purified protein derivative-activated type 1 cytokine-producing $CD4^+$ T lymphocytes in the lung: a characteristic feature of active pulmonary and nonpulmonary tuberculosis. J. Infect. Dis. **187:**243–250.
5. **Basu, S., T. M. Schaefer, M. Ghosh, C. L. Fuller, and T. A. Reinhart.** 2002. Molecular cloning and sequencing of 25 different rhesus macaque chemokine cDNAS reveals evolutionary conservation among C, CC, CXC, and CX3C families of chemokines. Cytokine **18:**140–148.
6. **Bean, A. G., D. R. Roach, H. Briscoe, M. P. France, H. Korner, J. D. Sedgwick, and W. J. Britton.** 1999. Structural deficiencies in granuloma formation in TNF gene-targeted mice underlie the heightened susceptibility to aerosol *Mycobacterium tuberculosis* infection, which is not compensated for by lymphotoxin. J. Immunol. **162:**3504–3511.
7. **Belasco, J. G., G. Nilsson, A. von Gabain, and S. N. Cohen.** 1986. The stability of *E. coli* gene transcripts is dependent on determinants localized to specific mRNA segments. Cell **46:**245–251.
8. **Belli, F., A. Capra, A. Moraiti, S. Rossi, and P. Rossi.** 2000. Cytokines assay in peripheral blood and bronchoalveolar lavage in the diagnosis and staging of pulmonary granulomatous diseases. Int. J. Immunopathol. Pharmacol. **13:**61–67.
9. **Bergeron, A., M. Bonay, M. Kambouchner, D. Lecossier, M. Riquet, P. Soler, A. Hance, and A. Tazi.** 1997. Cytokine patterns in tuberculous and sarcoid granulomas: correlations with histopathologic features of the granulomatous response. J. Immunol. **159:**3034–3043.
10. **Boros, D. L.** 1978. Granulomatous inflammations. Prog. Allergy **24:**183–267.
11. **Capuano, S., III, D. A. Croix, S. Pawar, A. Zinovik, A. Myers, P. L. Lin, S. Bissel, C. Fuhrman, E. Klein, and J. L. Flynn.** 2003. Experimental *Mycobacterium tuberculosis* infection of cynomolgus macaques closely resembles the various manifestations of human *M. tuberculosis* infection. Infect. Immun. **71:**5831–5844.
12. **Chensue, S. W., K. Warmington, J. Ruth, P. Lincoln, M. C. Kuo, and S. L. Kunkel.** 1994. Cytokine responses during mycobacterial and schistosomal antigen-induced pulmonary granuloma formation. Production of Th1 and Th2 cytokines and relative contribution of tumor necrosis factor. Am. J. Pathol. **145:**1105–1113.
13. **Chensue, S. W., K. S. Warmington, J. H. Ruth, P. Lincoln, and S. L. Kunkel.** 1995. Cytokine function during mycobacterial and schistosomal antigen-induced pulmonary granuloma formation. Local and regional participation of IFN-gamma, IL-10, and TNF. J. Immunol. **154:**5969–5976.
14. **Chiu, B. C., C. M. Freeman, V. R. Stolberg, E. Komuniecki, P. M. Lincoln, S. L. Kunkel, and S. W. Chensue** 2003. Cytokine-chemokine networks in experimental mycobacterial and schistosomal lung granuloma formation. Am. J. Respir. Cell Mol. Biol. **29:**106–116.
15. **Choi, Y. K., B. A. Fallert, M. A. Murphey-Corb, and T. A. Reinhart.** 2003. Simian immunodeficiency virus dramatically alters expression of homeostatic chemokines and dendritic cell markers during infection in vivo. Blood **101:**1684–1691.
16. **Cooper, A. M., D. K. Dalton, T. A. Stewart, J. P. Griffin, D. G. Russell, and I. M. Orme.** 1993. Disseminated tuberculosis in interferon gamma gene-disrupted mice. J. Exp. Med. **178:**2243–2247.
17. **D'Ambrosio, D., M. Mariani, P. Panina-Bordignon, and F. Sinigaglia.** 2001. Chemokines and their receptors guiding T lymphocyte recruitment in lung inflammation. Am. J. Respir. Crit. Care Med. **164:**1266–1275.
18. **Dixon, A. E., J. B. Mandac, D. K. Madtes, P. J. Martin, and J. G. Clark.** 2000. Chemokine expression in Th1 cell-induced lung injury: prominence of IFN-gamma-inducible chemokines. Am. J. Physiol. Lung Cell Mol. Physiol. **279:**L592–L599.
19. **Dye, C., S. Scheele, P. Dolin, V. Pathania, and M. C. Raviglione.** 1999. Consensus statement. Global burden of tuberculosis: estimated incidence, prevalence, and mortality by country. W. H. O. Global Surveillance and Monitoring Project. JAMA **282:**677–686.
20. **Fallert, B. A., and T. A. Reinhart.** 2002. Improved detection of simian immunodeficiency virus RNA by in situ hybridization in fixed tissue sections: combined effects of temperatures for tissue fixation and probe hybridization. J. Virol. Methods **99:**23–32.
21. **Fenhalls, G., L. Stevens, L. Moses, J. Bezuidenhout, J. C. Betts, P. P. Helden, P. T. Lukey, and K. Duncan.** 2002. In situ detection of *Mycobacterium tuberculosis* transcripts in human lung granulomas reveals differential gene expression in necrotic lesions. Infect. Immun. **70:**6330–6338.
22. **Fenhalls, G., L. Stevens-Muller, R. Warren, N. Carroll, J. Bezuidenhout, P. van Helden, and P. Bardin.** 2002. Localisation of mycobacterial DNA and mRNA in human tuberculous granulomas. J. Microbiol. Methods **51:**197–208.
23. **Fenhalls, G., A. Wong, J. Bezuidenhout, P. van Helden, P. Bardin, and P. T. Lukey.** 2000. In situ production of gamma interferon, interleukin-4, and tumor necrosis factor alpha mRNA in human lung tuberculous granulomas. Infect. Immun. **68:**2827–2836.
24. **Ferrero, E., P. Biswas, K. Vettoretto, M. Ferrarini, M. Uguccioni, L. Piali, B. E. Leone, B. Moser, C. Rugarli, and R. Pardi.** 2003. Macrophages exposed to *Mycobacterium tuberculosis* release chemokines able to recruit selected leucocyte subpopulations: focus on gamma delta cells. Immunology **108:**365–374.
25. **Flynn, J. L., J. Chan, K. J. Triebold, D. K. Dalton, T. A. Stewart, and B. R.**

Bloom. 1993. An essential role for interferon gamma in resistance to *Mycobacterium tuberculosis* infection. J. Exp. Med. **178:**2249–2254.
26. **Foxman, E. F., J. J. Campbell, and E. C. Butcher.** 1997. Multistep navigation and the combinatorial control of leukocyte chemotaxis. J. Cell Biol. **139:** 1349–1360.
27. **Fukunaga, H., T. Murakami, T. Gondo, K. Sugi, and T. Ishihara.** 2002. Sensitivity of acid-fast staining for *Mycobacterium tuberculosis* in formalin-fixed tissue. Am. J. Respir. Crit. Care Med. **166:**994–997.
28. **Gangur, V., F. E. Simons, and K. T. Hayglass.** 1998. Human IP-10 selectively promotes dominance of polyclonally activated and environmental antigen-driven IFN-gamma over IL-4 responses. FASEB J. **12:**705–713.
29. **Jouanguy, E., F. Altare, S. Lamhamedi, P. Revy, J. F. Emile, M. Newport, M. Levin, S. Blanche, E. Seboun, A. Fischer, and J. L. Casanova.** 1996. Interferon-gamma-receptor deficiency in an infant with fatal bacille Calmette-Guerin infection. N. Engl. J. Med. **335:**1956–1961.
30. **Kaufmann, S. H.** 2001. How can immunology contribute to the control of tuberculosis? Nat. Rev. Immunol. **1:**20–30.
31. **Kaufmann, S. H.** 2002. Protection against tuberculosis: cytokines, T cells, and macrophages. Ann. Rheum. Dis. **61**(Suppl. 2)**:**ii54–ii58.
32. **Kawahara, M., T. Nakasone, and M. Honda.** 2002. Dynamics of gamma interferon, interleukin-12 (IL-12), IL-10, and transforming growth factor beta mRNA expression in primary *Mycobacterium bovis* BCG infection in guinea pigs measured by a real-time fluorogenic reverse transcription-PCR assay. Infect. Immun. **70:**6614–6620.
33. **Lande, R., E. Giacomini, T. Grassi, M. E. Remoli, E. Iona, M. Miettinen, I. Julkunen, and E. M. Coccia.** 2003. IFN-alpha beta released by *Mycobacterium tuberculosis*-infected human dendritic cells induces the expression of CXCL10: selective recruitment of NK and activated T cells. J. Immunol. **170:**1174–1182.
34. **Langermans, J. A., P. Andersen, D. van Soolingen, R. A. Vervenne, P. A. Frost, T. van der Laan, L. A. van Pinxteren, J. van den Hombergh, S. Kroon, I. Peekel, S. Florquin, and A. W. Thomas.** 2001. Divergent effect of bacillus Calmette-Guerin (BCG) vaccination on *Mycobacterium tuberculosis* infection in highly related macaque species: implications for primate models in tuberculosis vaccine research. Proc. Natl. Acad. Sci. USA **98:**11497–11502.
35. **Luster, A. D.** 1998. Chemokines—chemotactic cytokines that mediate inflammation. N. Engl. J. Med. **338:**436–445.
36. **Mariano, M.** 1995. The experimental granuloma. A hypothesis to explain the persistence of the lesion. Rev. Inst. Med. Trop. Sao Paulo **37:**161–176.
37. **Means, T. K., S. Wang, E. Lien, A. Yoshimura, D. T. Golenbock, and M. J. Fenton.** 1999. Human toll-like receptors mediate cellular activation by *Mycobacterium tuberculosis*. J. Immunol. **163:**3920–3927.
38. **Murray, P. J.** 1999. Defining the requirements for immunological control of mycobacterial infections. Trends Microbiol. **7:**366–372.
39. **Newport, M. J., C. M. Huxley, S. Huston, C. M. Hawrylowicz, B. A. Oostra, R. Williamson, and M. Levin.** 1996. A mutation in the interferon-gamma-receptor gene and susceptibility to mycobacterial infection. N. Engl. J. Med. **335:**1941–1949.
40. **Orme, I. M.** 1998. The immunopathogenesis of tuberculosis: a new working hypothesis. Trends Microbiol. **6:**94–97.
41. **Orme, I. M., and A. M. Cooper.** 1999. Cytokine/chemokine cascades in immunity to tuberculosis. Immunol. Today **20:**307–312.
42. **Park, M. K., D. Amichay, P. Love, E. Wick, F. Liao, A. Grinberg, R. L. Rabin, H. H. Zhang, S. Gebeyehu, T. M. Wright, A. Iwasaki, Y. Weng, J. A. De Martino, K. L. Elkins, and J. M. Farber.** 2002. The CXC chemokine murine monokine induced by IFN-gamma (CXC chemokine ligand 9) is made by APCs, targets lymphocytes including activated B cells, and supports antibody responses to a bacterial pathogen in vivo. J. Immunol. **169:**1433–1443.
43. **Patel, S., M. Yates, and N. A. Saunders.** 1997. PCR-enzyme-linked immunosorbent assay and partial rRNA gene sequencing: a rational approach to identifying mycobacteria. J. Clin. Microbiol. **35:**2375–2380.
44. **Proost, P., E. Schutyser, P. Menten, S. Struyf, A. Wuyts, G. Opdenakker, M. Detheux, M. Parmentier, C. Durinx, A. M. Lambeir, J. Neyts, S. Liekens, P. C. Maudgal, A. Billiau, and J. Van Damme.** 2001. Amino-terminal truncation of CXCR3 agonists impairs receptor signaling and lymphocyte chemotaxis, while preserving antiangiogenic properties. Blood **98:**3554–3561.
45. **Qiu, B., K. A. Frait, F. Reich, E. Komuniecki, and S. W. Chensue.** 2001. Chemokine expression dynamics in mycobacterial (type-1) and schistosomal (type-2) antigen-elicited pulmonary granuloma formation. Am. J. Pathol. **158:**1503–1515.
46. **Reinhart, T. A., B. A. Fallert, M. E. Pfeifer, S. Sanghavi, S. Capuano III, P. Rajakumar, M. Murphey-Corb, R. Day, C. L. Fuller, and T. M. Schaefer.** 2002. Increased expression of the inflammatory chemokine CXC chemokine ligand 9/monokine induced by interferon-gamma in lymphoid tissues of rhesus macaques during simian immunodeficiency virus infection and acquired immunodeficiency syndrome. Blood **99:**3119–3128.
47. **Rhoades, E. R., A. M. Cooper, and I. M. Orme.** 1995. Chemokine response in mice infected with *Mycobacterium tuberculosis*. Infect. Immun. **63:**3871–3877.
48. **Roach, D. R., A. G. Bean, C. Demangel, M. P. France, H. Briscoe, and W. J. Britton.** 2002. TNF regulates chemokine induction essential for cell recruitment, granuloma formation, and clearance of mycobacterial infection. J. Immunol. **168:**4620–4627.
49. **Roach, D. R., H. Briscoe, K. Baumgart, D. A. Rathjen, and W. J. Britton.** 1999. Tumor necrosis factor (TNF) and a TNF-mimetic peptide modulate the granulomatous response to *Mycobacterium bovis* BCG infection in vivo. Infect. Immun. **67:**5473–5476.
50. **Robinson, D. S., S. Ying, I. K. Taylor, A. Wangoo, D. M. Mitchell, A. B. Kay, Q. Hamid, and R. J. Shaw.** 1994. Evidence for a Th1-like bronchoalveolar T-cell subset and predominance of interferon-gamma gene activation in pulmonary tuberculosis. Am. J. Respir. Crit. Care Med. **149:**989–993.
51. **Romagnani, P., F. Annunziato, E. Lazzeri, L. Cosmi, C. Beltrame, L. Lasagni, G. Galli, M. Francalanci, R. Manetti, F. Marra, V. Vanini, E. Maggi, and S. Romagnani.** 2001. Interferon-inducible protein 10, monokine induced by interferon gamma, and interferon-inducible T-cell alpha chemoattractant are produced by thymic epithelial cells and attract T-cell receptor (TCR) alphabeta$^+$ CD8$^+$ single-positive T cells, TCRgammadelta$^+$ T cells, and natural killer-type cells in human thymus. Blood **97:**601–607.
52. **Sallusto, F., D. Lenig, C. R. Mackay, and A. Lanzavecchia.** 1998. Flexible programs of chemokine receptor expression on human polarized T helper 1 and 2 lymphocytes. J. Exp. Med. **187:**875–883.
53. **Saunders, B. M., and A. M. Cooper.** 2000. Restraining mycobacteria: role of granulomas in mycobacterial infections. Immunol. Cell Biol. **78:**334–341.
54. **Sauty, A., R. A. Colvin, L. Wagner, S. Rochat, F. Spertini, and A. D. Luster.** 2001. CXCR3 internalization following T cell-endothelial cell contact: preferential role of IFN-inducible T cell alpha chemoattractant (CXCL11). J. Immunol. **167:**7084–7093.
55. **Somoskovi, A., G. Zissel, P. F. Zipfel, M. W. Ziegenhagen, J. Klaucke, H. Haas, M. Schlaak, and J. Muller-Quernheim.** 1999. Different cytokine patterns correlate with the extension of disease in pulmonary tuberculosis. Eur. Cytokine Netw. **10:**135–142.
56. **Taha, R. A., T. C. Kotsimbos, Y. L. Song, D. Menzies, and Q. Hamid.** 1997. IFN-gamma and IL-12 are increased in active compared with inactive tuberculosis. Am. J. Respir. Crit. Care Med. **155:**1135–1139.
57. **Taha, R. A., E. M. Minshall, R. Olivenstein, D. Ihaku, B. Wallaert, A. Tsicopoulos, A. B. Tonnel, R. Damia, D. Menzies, and Q. A. Hamid.** 1999. Increased expression of IL-12 receptor mRNA in active pulmonary tuberculosis and sarcoidosis. Am. J. Respir. Crit. Care Med. **160:**1119–1123.
58. **Underhill, D. M., A. Ozinsky, K. D. Smith, and A. Aderem.** 1999. Toll-like receptor-2 mediates mycobacteria-induced proinflammatory signaling in macrophages. Proc. Natl. Acad. Sci. USA **96:**14459–14463.
59. **van Crevel, R., T. H. Ottenhoff, and J. W. van der Meer.** 2002. Innate immunity to *Mycobacterium tuberculosis*. Clin. Microbiol. Rev. **15:**294–309.
60. **Van Damme, J., S. Struyf, A. Wuyts, E. Van Coillie, P. Menten, D. Schols, S. Sozzani, I. De Meester, and P. Proost.** 1999. The role of CD26/DPP IV in chemokine processing. Chem. Immunol. **72:**42–56.
61. **von Gabain, A., J. G. Belasco, J. L. Schottel, A. C. Chang, and S. N. Cohen.** 1983. Decay of mRNA in *Escherichia coli*: investigation of the fate of specific segments of transcripts. Proc. Natl. Acad. Sci. USA **80:**653–657.
62. **Walsh, G. P., E. V. Tan, E. C. dela Cruz, R. M. Abalos, L. G. Villahermosa, L. J. Young, R. V. Cellona, J. B. Nazareno, and M. A. Horwitz.** 1996. The Philippine cynomolgus monkey (*Macaca fasicularis*) provides a new nonhuman primate model of tuberculosis that resembles human disease. Nat. Med. **2:**430–436.

Editor: S. H. E. Kaufmann